

Blue Photoluminescence from Chemically Derived Graphene Oxide

By Goki Eda, Yun-Yue Lin, Cecilia Mattevi, Hisato Yamaguchi, Hsin-An Chen, I-Sheng Chen, Chun-Wei Chen,* and Manish Chhowalla*

Fluorescent organic compounds are of significant importance to the development of low-cost opto-electronic devices.^[1] Blue fluorescence from aromatic or olefinic molecules and their derivatives is particularly important for display and lighting applications.^[2] Thin-film deposition of low-molecular-weight, fluorescent organic compounds typically requires costly vacuum evaporation systems. On the other hand, solution-processable polymeric counterparts generally exhibit luminescence at longer wavelengths due to larger delocalization in the chain. Blue-light emission from solution-processed materials is therefore of unique technologic significance. Here, we report near-UV-to-blue photoluminescence (PL) from solution-processed graphene oxide (GO). The characteristics of the PL and its dependence on the reduction of GO indicates that it originates from the recombination of electron–hole (e–h) pairs, localized within small sp^2 carbon clusters embedded within an sp^3 matrix. The results suggest that a sheet of graphene provides a parent structure on which fluorescent components can be chemically engineered without losing the macroscopic structural integrity. Our findings offer a unique route towards solution-processable opto-electronics devices with graphene.

Graphene is an exciting material for fundamental and applied solid-state physics research.^[3] Novel condensed-matter effects, arising from its unique 2D energy dispersion along with superior properties, are promising towards a wide variety of applications. However, graphene is a zero-bandgap semiconductor, which creates a unique set of challenges for implementation into conventional electronics due to substantial leakage currents in field-effect devices.^[4] Due to the lack of a bandgap the possibility of observing luminescence is also highly unlikely.

Recently, chemically derived GO has been receiving attention for large-area electronics because its solubility in a variety of solvents allows ease of wafer-scale deposition.^[5–11] Transport of carriers in reduced GO is limited by the structural disorder.^[12,13] However, conductivity of $\sim 10^5 \text{ S m}^{-1}$ (Ref. [5,6,14]) and mobilities

of $\sim 10 \text{ cm}^2 \text{ V s}^{-1}$ (Ref. [15]) are sufficiently large for applications where inexpensive and moderate performance electronics (such as on flexible platforms) are required. In GO, a large fraction (0.5–0.6) of carbon is sp^3 hybridized and covalently bonded with oxygen in form of epoxy and hydroxyl groups.^[16,17] The remaining carbon is sp^2 hybridized and bonded either with neighboring carbon atoms or with oxygen in the form of carboxyl and carbonyl groups, which predominantly decorate the edges of the graphene sheets. GO is therefore a 2D network of sp^2 - and sp^3 -bonded atoms, in contrast to an ideal graphene sheet, which consists of 100% sp^2 -hybridized carbon atoms. This unique atomic and electronic structure of GO,^[18] consisting of variable sp^2/sp^3 fractions, opens up possibilities for new functionalities. The most notable difference between GO and mechanically exfoliated graphene is the optoelectronic properties arising from the presence of a finite bandgap.^[19] Recently, PL from chemically derived GO has been demonstrated.^[20–22] The luminescence of GO was found to occur in the visible (vis) and near-infrared (IR) wavelengths range, a property useful for biosensing and fluorescence tags.^[20,21]

In carbon materials containing a mixture of sp^2 and sp^3 bonding, the opto-electronic properties are determined by the π states of the sp^2 sites.^[23] The π and π^* electronic levels of the sp^2 clusters lie within the bandgap of σ and σ^* states of the sp^3 matrix and are strongly localized.^[24,25] The optical properties of disordered carbon thin films containing a mixture of sp^2 and sp^3 carbon have been widely investigated.^[26–30] The PL in such carbon systems is a consequence of geminate recombination of localized e–h pairs in sp^2 clusters, which essentially behave as the luminescence centers or chromophores.^[31] Since the bandgap depends on the size, shape, and fraction of the sp^2 domains, tunable PL emission can be achieved by controlling the nature of sp^2 sites. For example, PL energy linearly scales with the sp^2 fraction in disordered carbon systems.^[32]

Here we demonstrate that moderately reduced GO thin films consisting of several monolayers emitting near-UV blue light when excited with UV radiation. The blue PL was observed for thin-film samples deposited from thoroughly exfoliated suspensions. We also observed red and near-IR emission, comparable to Reference [20–22] (see Supporting Information), on GO films drop-casted from poorly dispersed suspensions. We demonstrate that by appropriately controlling the concentration of isolated sp^2 clusters through reduction treatment, the PL intensity can be increased by a factor of 10 compared to the as-synthesized material. Reduction of GO can be achieved in a number of ways to obtain graphene-like electrically conductive material.^[11] A common reduction method is exposure to hydrazine vapor,

[*] Prof. M. Chhowalla,^[+] Dr. C. Mattevi,^[+] Dr. H. Yamaguchi, G. Eda,^[+] Materials Science and Engineering, Rutgers University
607 Taylor Road, Piscataway, NJ 08854 (USA)
E-mail: manish1@rci.rutgers.edu

Prof. C.-W. Chen, Y.-Y. Lin, H.-A. Chen, I.-S. Chen
Materials Science and Engineering, National Taiwan University
No. 1, Sec. 4, Roosevelt Road, Taipei 10617 (Taiwan)

[+] Present address: Department of Materials, Imperial College,
Exhibition Road, London SW7 2AZ (UK)
E-mail: chunwei@ntu.edu.tw

DOI: 10.1002/adma.200901996

which leads to the transformation of GO from an insulator to a semimetal.^[7] The gradual transformation of GO is confirmed by absorbance measurements, shown in Figure 1a, on the same film at various stages of reduction (i.e., hydrazine-vapor exposure time). The main absorbance peak attributed to π - π^* transitions of C=C in as-synthesized GO occurs at around ~ 200 nm, which red shifts to ~ 260 nm upon reduction. The broad absorption spectra that extend up to 1500 nm indicate the absence of a well-defined bandedge in the UV-vis energy range. A shoulder around 320 nm observed for as-synthesized GO may be attributed to n - π^* transitions of C=O.^[33] This shoulder disappears almost immediately after exposure to hydrazine treatment (see Supporting Information), most likely due to the decrease in the concentration of carboxyl groups. The absorbance is found to

increase with hydrazine exposure time, consistent with the evolution of oxygen (from ~ 39 at.% in starting GO to 7–8 at.% in the reduced GO) and a concomitant increase in the sp^2 fraction from 0.4 to 0.8.^[14,17]

The corresponding PL spectra of the GO thin film after each incremental hydrazine-vapor exposure (from 20 s up to 60 min) are shown in Figure 1b. It is immediately clear that in contrast to the broad absorption features, a relatively narrow PL peak (FWHM ~ 0.6 eV) centered around 390 nm is observed. The liquid suspensions of GO used for the film deposition exhibited an apparently equivalent PL peak centered around 440 nm (see Supporting Information). The shift in the suspension PL can be attributed to the difference in the dielectric environment.^[34] The PL intensity was weak but visible by unaided eyes for excitation conditions used in this study. Preliminary measurements have indicated that the quantum yield is also very low but a detailed study of the quantum efficiency will be presented elsewhere. The PL signal, however, was sufficiently strong to allow reproducible data collection using the described measurement conditions.

The PL peak positions of the thin films were found to remain constant around ~ 390 nm with reduction treatment, varying by less than ± 10 nm. It can be seen that while the PL intensity is weak for as-deposited GO films, short exposure to hydrazine vapor results in a dramatic increase in the PL intensities. Interestingly, this trend is reversed after >3 min exposure to hydrazine vapor. Longer exposure leads to eventual quenching of the PL signal. It should be mentioned that reduction by thermal annealing at 200°C in vacuum also led to weaker PL signal (see Supporting Information). The PL excitation spectra at different PL emission wavelengths for a GO film reduced for 3 min are shown in Figure 1c. Excitonic features are readily observable between excitation wavelengths of 260 and 310 nm ($4\sim 4.4$ eV), which represent the absorption energies corresponding to emission of blue light. The general features of the PL emission/excitation spectra and their dependence on the degree of reduction are markedly different from the red-IR emission reported in previous studies,^[20–22] suggesting that the origin of the blue emission is also different. It should be noted that for the observation of UV-blue PL, it is necessary to minimize the concentration of multilayered and aggregated flakes via centrifugation. Since we observed red-near-IR PL from GO suspensions prior to centrifugation, we suspect that low-energy PL can be attributed to the presence of such particles, in which interlayer electronic relaxation can occur.

One possible origin of the blue PL is the radiative recombination of e - h pairs generated within localized states. The energy gap between the π and π^* states generally depends on the size of sp^2 clusters^[23] or conjugation length.^[35] From Raman and imaging analysis, it has been suggested that GO consists of ~ 3 nm sp^2 clusters isolated within sp^3 carbon matrix.^[12,14,18] Although no direct observation of “molecular” sp^2 domains has been reported, our transport studies in progressively reduced GO^[14,36] and previous works on PL from amorphous carbons^[28,37,38] suggest their presence. It is the interactions between the nanometer-size sp^2 clusters and the finite-sized molecular sp^2 domains that is the key in optimizing the blue emission in GO. The sp^2 clusters with a diameter of ~ 3 nm consist of >100 aromatic rings. Our calculations based on Gaussian and time-dependent (TD) density functional theory (DFT) calculations

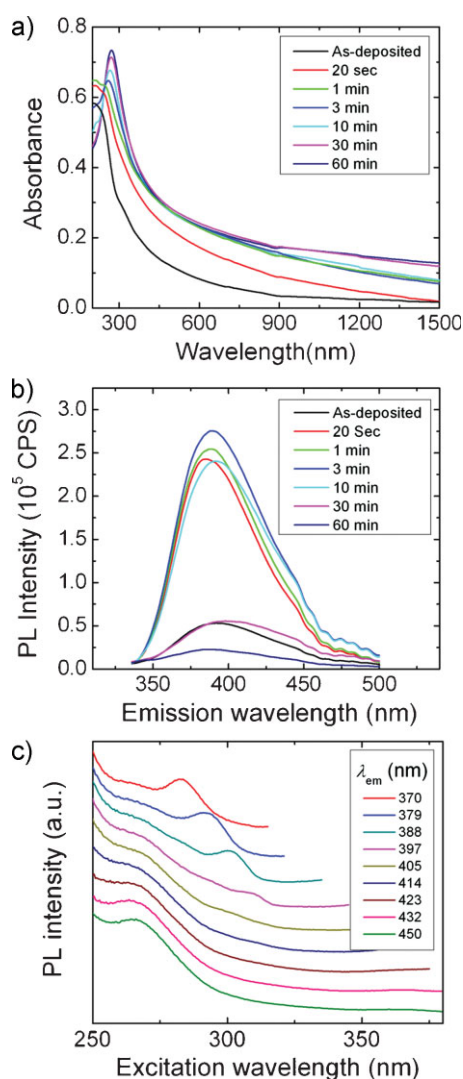


Figure 1. a) Absorbance and b,c) photoluminescence spectra of progressively reduced GO thin films. The total time of exposure to hydrazine is noted in the legend. The photoluminescence spectra in (b) were obtained for excitation at 325 nm. The PL excitation spectra in (c) were obtained for different wavelengths of the emission spectrum ranging from 370 to 450 nm.

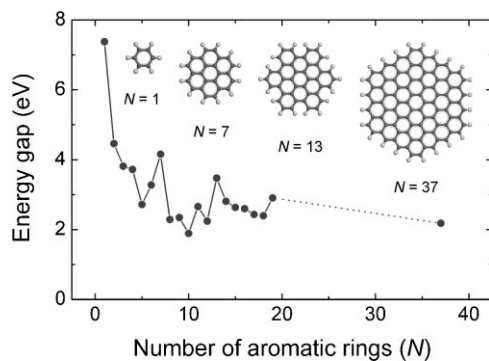


Figure 2. Energy gap of π - π^* transitions calculated based on DFT as a function of the number of fused aromatic rings (N). The inset shows the structures of the graphene molecules used for calculation.

(see Supporting Information for details) indicate that such sp^2 clusters have energy gaps of around 0.5 eV and cannot be responsible for the blue emission observed here. Figure 2 shows that the calculated gap between the highest occupied molecular orbital (HOMO) and the lowest unoccupied molecular orbital (LUMO) of a single benzene ring is ~ 7 eV, which decreases down to ~ 2 eV for a cluster of 20 aromatic rings. Thus, we expect that much smaller sp^2 clusters of few aromatic rings or of some other sp^2 configuration of similar size are likely to be responsible for the observed blue PL. Our previously proposed structural model for GO takes into account both the larger sp^2 domains and also the smaller sp^2 fragments that are responsible for the transport of carriers between the larger sp^2 domains.^[14] In this view, the observed increase in the PL intensity without energy shift during the initial reduction treatments may be attributed to the increased concentration of such sp^2 fragments. Furthermore, the subsequent PL quenching with longer reduction may be the result of percolation among these sp^2 configurations, facilitating transport of excitons to nonradiative recombination sites.

To test this hypothesis, we investigated the electrical transport properties of individual sheets of GO, progressively reduced by exposure to hydrazine. We have recently shown that electrical properties of GO are sensitively dependent on sp^2 -carbon fractions and the spatial distribution of the smaller domains, serving as an indirect probe for the structural information regarding the evolution of the sp^2 phase with reduction.^[14,36] Figure 3a shows the I - V characteristics of an identical GO device reduced at different levels. It can be seen that the low-bias current is suppressed in GO that was reduced for 2 min, whereas a dramatic increase in current is observed after 5 min of reduction. The conduction is dominated by tunneling for GO reduced for 2 min while hopping begins to contribute to conduction after longer reduction (>5 min) (see Ref. [36] for a complete study of transport in progressively reduced GO). The transfer characteristics of these devices further indicate that GO essentially remains an insulator after 2 min of exposure to hydrazine vapor (Fig. 3b). After 5 min of reduction, an ambipolar field effect becomes observable albeit with low current. These trends observed in the electrical properties are in striking contrast to the optical properties presented in Figure 1a and 1b. The general trends in absorbance, PL intensity, and electrical conductivity with

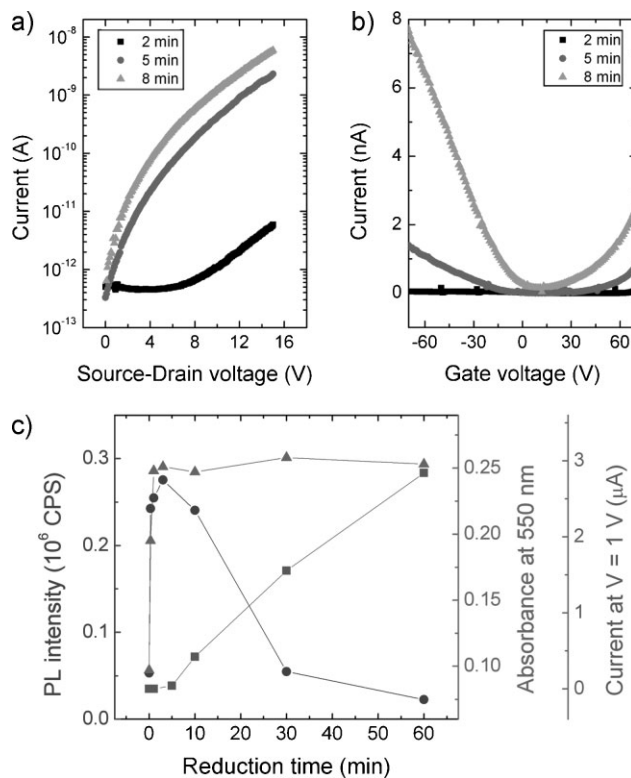


Figure 3. a) I - V and b) transfer characteristics of individual GO sheet devices at different stages of reduction. The total time of exposure to hydrazine is noted in the legend. c) Summary plot showing the maximum PL intensity (circles), absorbance at 550 nm (triangles), and current at 1 V (squares) of a GO thin film as a function of reduction time.

reduction time are summarized in Figure 3c. It can be noticed that the initial rapid rise of the PL intensity is coupled with the absorbance behavior, while the gradual quenching can be correlated with a gradual increase in the conductivity. That is, while the absorbance of GO thin films increases immediately after only 20 s of exposure to hydrazine vapor, the electrical conductivity remains low.

These results are consistent with our hypothesis that at the initial stages of reduction process, the fraction of strongly localized sp^2 sites increases, thereby improving absorbance and PL intensity, while the energetic coupling between these sites remains negligibly small. Recent photoconductivity studies also indicate that e-h pairs can be photogenerated and dissociated under relatively large electric field (>400 V cm^{-1}) in reduced GO films.^[39] In the later stages of the reduction process, interconnectivity of the localized sp^2 sites increases, thereby facilitates hopping of excitons to nonradiative recombination centers, and consequently quenches PL. Based on these observations, we have refined our previous structural model for GO at different stages of reduction to explain the PL results as shown in Figure 4. Figure 4a shows a schematic representation of the structure of as-prepared GO containing ~ 3 nm sp^2 clusters (not drawn to scale), along with smaller sp^2 configurations dispersed in an insulating sp^3 matrix, where a large fraction of carbon is bonded with oxygen (oxygen atoms are represented by grey dots). Initially, the

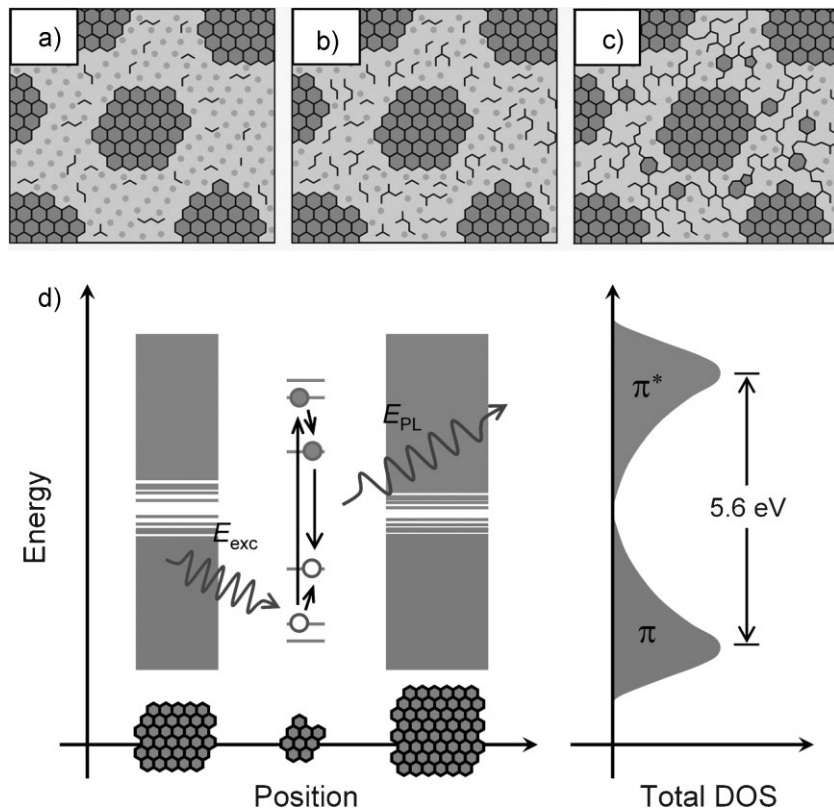


Figure 4. a–c) Structural models of GO at different stages of reduction. The larger sp^2 clusters of aromatic rings are not drawn to scale. The smaller sp^2 domains indicated by zigzag lines do not necessarily correspond to any specific structure (such as olefinic chains for example) but to small and localized sp^2 configurations that act as the luminescence centers. The PL intensity is relatively weak for (a) as-synthesized GO but increases with reduction due to (b) formation of additional small sp^2 domains between the larger clusters because of evolution of oxygen with reduction. After extensive reduction, the smaller sp^2 domains create (c) percolating pathways among the larger clusters. d) Representative band structure of GO. The energy levels are quantized with large energy gap for small fragments due to confinement. A photogenerated e–h pair recombining radiatively is depicted.

concentration of smaller sp^2 domains is low, yielding moderate PL emission. In Figure 4b, the evolution of the smaller sp^2 domains due to the removal of some oxygen with reduction is shown. Based on our previous study,^[14] we have found that the dimensions of the larger sp^2 clusters do not change but that the transport is mediated by the increase in concentration and size of the smaller sp^2 domains. The formation of new isolated smaller domains consisting of few conjugated repeating units, as shown in Figure 4b, results in the enhancement of the PL intensity observed between 20 s and 3 min of reduction. Further removal of oxygen by continued exposure to hydrazine vapor leads to percolation between the larger sp^2 clusters via growth of smaller sp^2 domains, as shown in Figure 4c. Based on the simple particle-in-a-box argument, it can be readily surmised that the PL from the structure shown in Figure 4c is likely to be significantly quenched, as observed in Figure 1b. It has been suggested that the nonradiative lifetime of e–h pairs govern the experimental PL decay times.^[31] The above argument is further supported by our time-resolve PL measurements (see Supporting Information), which show shorter decay times for GO films reduced for more

than 3 min. The band diagram corollary of the physical picture is represented in Figure 4d, where the blue PL from excitation and recombination among the discrete energy levels of small sp^2 fragments is represented. The energy states are highly localized due to the large $\sigma-\sigma^*$ gap of the sp^3 matrix (not shown in schematics), which is expected to be of the order of ~ 6 eV.^[23] The large sp^2 clusters (~ 3 nm) have energy gaps that are lower than those of the smaller sp^2 fragments and largely determine the total electronic density of states (DOS) of the material. The excitation and recombination in discrete energy states and the larger gap of the small fragments, as shown in Figure 4d, are likely to be responsible for the enhanced blue PL emission in slightly reduced GO.

In summary, we describe blue PL from chemically derived GO thin films deposited from thoroughly exfoliated suspensions. The presence of isolated sp^2 clusters within the carbon–oxygen sp^3 matrix leads to the localization of e–h pairs, facilitating radiative recombination of small clusters. The PL intensity was found to vary with reduction treatment, which can be correlated to the evolution of very small sp^2 clusters. Our calculations suggest that sp^2 clusters of several conjugated repeating units yield bandgaps consistent with blue emission. The overall intensity of PL was moderate due to the lower total cross-section of emitting molecular sp^2 -domain centers relative to nonradiative recombination sites. The possibility of engineering desired molecular sp^2 structures in graphene via controlled oxidation to achieve highly efficient and tunable PL will be important towards the exploitation of blue PL for optoelectronics applications. These

results inspire further experiments based on temperature dependence of PL for better clarification of the electronic processes occurring in GO.

Acknowledgements

This research funded by the NSF CAREER Award (ECS 0543867). We acknowledge financial support from the Rutgers University Academic Excellence Fund and Institute for Advanced Materials, Devices, and Nanotechnology (IAMDN). The authors thank Mr. Wei-Jung Lai at the Center for Condensed Matter Sciences, NTU, for assistance with PLE measurements. Supporting Information is available online from Wiley InterScience or from the author.

Received: June 14, 2009

Revised: July 27, 2009

Published online:

[1] J. R. Sheats, H. Antoniadis, M. Hueschen, W. Leonard, J. Miller, R. Moon, D. Roitman, A. Stocking, *Science* **1996**, 273, 884.

[2] L. J. Rothberg, A. J. Lovinger, *J. Mater. Res.* **1996**, 11, 3174.

- [3] A. K. Geim, K. S. Novoselov, *Nat. Mater.* **2007**, *6*, 183.
- [4] K. S. Novoselov, A. K. Geim, S. V. Morozov, D. Jiang, Y. Zhang, S. V. Dubonos, I. V. Grigorieva, A. A. Firsov, *Science* **2004**, *306*, 666.
- [5] X. Wang, L. Zhi, K. Mullen, *Nano Lett.* **2007**, *8*, 323.
- [6] H. A. Becerill, J. Mao, Z. Liu, R. M. Stoltenberg, Z. Bao, Y. Chen, *ACS Nano* **2008**, *2*, 463.
- [7] G. Eda, G. Fanchini, M. Chhowalla, *Nat. Nanotechnol.* **2008**, *3*, 270.
- [8] J. T. Robinson, F. K. Perkins, E. S. Snow, Z. Wei, P. E. Sheehan, *Nano Lett.* **2008**, *8*, 3137.
- [9] J. T. Robinson, M. Zalalutdinov, J. W. Baldwin, E. S. Snow, Z. Wei, P. Sheehan, B. H. Houston, *Nano Lett.* **2008**, *8*, 3441.
- [10] G. Eda, Y.-Y. Lin, S. Miller, C.-W. Chen, W.-F. Su, M. Chhowalla, *Appl. Phys. Lett.* **2008**, *92*, 233305.
- [11] S. Park, R. S. Ruoff, *Nat. Nanotechnol.* **2009**, *4*, 217.
- [12] C. Gomez-Navarro, T. R. Weitz, A. M. Bittner, M. Scolari, A. Mews, M. Burghard, K. Kern, *Nano Lett.* **2007**, *7*, 3499.
- [13] A. B. Kaiser, C. Gomez-Navarro, R. S. Sundaram, M. Burghard, K. Kern, *Nano Lett.* **2009**, *9*, 1787.
- [14] C. Mattevi, G. Eda, S. Agnoli, S. Miller, K. A. Mkhoyan, O. Celik, D. Mastrogiovanni, G. Granozzi, E. Garfunkel, M. Chhowalla, *Adv. Funct. Mater.* **2009**, *19*, 1.
- [15] S. Wang, P.-J. Chia, L.-L. Chua, L.-H. Zhao, R.-Q. Png, S. Sivaramkrishnan, M. Zhou, R. G. S. Goh, R. H. Friend, A. T. S. Wee, P. K. H. Ho, *Adv. Mater.* **2008**, *20*, 3440.
- [16] W. Cai, R. D. Piner, F. J. Stadermann, S. Park, M. A. Shaibat, Y. Ishii, D. Yang, A. Velamakanni, S. J. An, M. Stoller, J. An, D. Chen, R. S. Ruoff, *Science* **2008**, *321*, 1815.
- [17] D. Yang, A. Velamakanni, G. Bozoklu, S. Park, M. Stoller, R. D. Piner, S. Stankovich, I. Jung, D. A. Field, C. A. Ventrice, Jr, R. S. Ruoff, *Carbon* **2009**, *47*, 145.
- [18] K. A. Mkhoyan, A. W. Contryman, J. Silcox, D. A. Stewart, G. Eda, C. Mattevi, S. Miller, M. Chhowalla, *Nano Lett.* **2009**, *9*, 1058.
- [19] D. W. Boukhvalov, M. I. Katsnelson, *J. Am. Chem. Soc.* **2008**, *130*, 10697.
- [20] X. Sun, Z. Liu, K. Welsher, J. T. Robinson, A. Goodwin, S. Zaric, H. Dai, *Nano Res.* **2008**, *1*, 203.
- [21] Z. Liu, J. T. Robinson, X. Sun, H. Dai, *J. Am. Chem. Soc.* **2008**, *130*, 10876.
- [22] Z. Zhengtang, M. V. Patrick, J. M. Eugene, A. T. C. Johnson, M. K. James, *Appl. Phys. Lett.* **2009**, *94*, 111909.
- [23] J. Robertson, E. P. O'Reilly, *Phys. Rev. B* **1987**, *35*, 2946.
- [24] C. Mathioudakis, G. Kopidakis, P. C. Kelires, P. Patsalas, M. Gioti, S. Logothetidis, *Thin Solid Films* **2005**, *482*, 151.
- [25] C. W. Chen, J. Robertson, *J. Non-Cryst. Solids* **1998**, *227*, 602.
- [26] J. Wagner, P. Lautenschlager, *J. Appl. Phys.* **1986**, *59*, 2044.
- [27] F. Demichelis, S. Schreiter, A. Tagliaferro, *Phys. Rev. B* **1995**, *51*, 2143.
- [28] Rusli, J. Robertson, G. A. J. Amaratunga, *J. Appl. Phys.* **1996**, *80*, 2998.
- [29] S. R. P. Silva, J. Robertson, Rusli, G. A. J. Amaratunga, J. Schwan, *Philos. Mag. B* **1996**, *74*, 369.
- [30] M. Koos, M. Fule, M. Veres, S. Toth, I. Pocsik, *Diamond Relat. Mater.* **2002**, *11*, 1115.
- [31] T. Heitz, C. Godet, J. G. Bouree, B. Drevillon, J. P. Conde, *Phys. Rev. B* **1999**, *60*, 6045.
- [32] J. Robertson, *Phys. Rev. B* **1996**, *53*, 16302.
- [33] Z. Luo, Y. Lu, L. A. Somers, A. T. C. Johnson, *J. Am. Chem. Soc.* **2009**, *131*, 898.
- [34] C. Jong Hyun, S. S. Michael, *Appl. Phys. Lett.* **2007**, *90*, 223114.
- [35] J. L. Bredas, R. Silbey, D. S. Boudreaux, R. R. Chance, *J. Am. Chem. Soc.* **1983**, *105*, 6555.
- [36] G. Eda, C. Mattevi, H. Yamaguchi, H. Kim, M. Chhowalla, *J. Phys. Chem. C* **2009**, *113*, 15768.
- [37] C. Godet, M. N. Berberan-Santos, *Diamond Relat. Mater.* **2001**, *10*, 168.
- [38] M. Koos, M. Veres, M. Fule, I. Pocsik, *Diamond Relat. Mater.* **2002**, *11*, 53.
- [39] X. Lv, Y. Huang, Z. Liu, J. Tian, Y. Wang, Y. Ma, J. Liang, S. Fu, X. Wan, Y. Chen, *Small* **2009**, *5*, 1682.